

Electronic Supplementary Information (ESI)

1. NMR related part

The peak positions of the two species mentioned in footnote ¶ are well known from the literature (Fig. ESI 1, left). The signal at lowest field is due to $[\text{Al}(\text{OH})_6\text{Mo}_6\text{O}_{18}]^{3-}$ (**a**) having an extremely high formation tendency (see: J.W. Akitt and A. Farthing, *J. Chem. Soc. Dalton Trans.*, 1981, 1615 and especially with a corrected formula L.-O. Öhman, *Inorg. Chem.* 1989, **28**, 3629; J.-H. Son, M. Choi and Y. U. Kwon, *J. Am. Chem. Soc.*, 2000, **122**, 7432), and the most upfield signal – always occurring in aqueous solutions of $\text{Al}_2(\text{SO}_4)_3$ – is assigned in the literature to $[\text{Al}(\text{H}_2\text{O})_5\text{SO}_4]^+$ (**b**) (J.W. Akitt and J.A. Farnsworth, *J. Chem. Soc., Faraday Trans 1*, 1985, **81(1)**, 193; J.W. Akitt, N.N. Greenwood and B.L. Khandelwal, *J. Chem. Soc. Dalton Trans.*, 1972, 1226) (for peak positions of **a** and **b** see Fig. 1 left below). Thus, there exist under the special conditions of the present investigation small but varying amounts of two additional products, due to a) either an aging process of **2a**, b) partial decomposition upon heating (note the high formation tendency of **a** due to the properties of “aggressive” Al^{3+} !), c) partial oxidation due to the addition of $\text{Al}(\text{NO}_3)_3$, or d) presence of small amounts of SO_4^{2-} and MoO_4^{2-} even in the crystal lattice. The latter anion – together with Al^{3+} – gives rise to the formation of **a** and the presence of sulphate to **b** (note the presence of Al^{3+} in solution). There seems to be the tendency of a slow reaction of the strongly polarizing Al^{3+} ions with the capsule especially upon heating to form **a**. (In this context it is important to note that the formation of **a** has – due to its high formation tendency – even been observed in the preparation of Mo catalysts on Al_2O_3 supports: X. Carrier, M. Che, *Appl. Catal. A: General* 2003, **253**, 317.) These types of decomposition scenarios do of course not occur in case of ions like Li^+ , Na^+ , K^+ etc. – being important for biomimetic studies – or lanthanide ions.

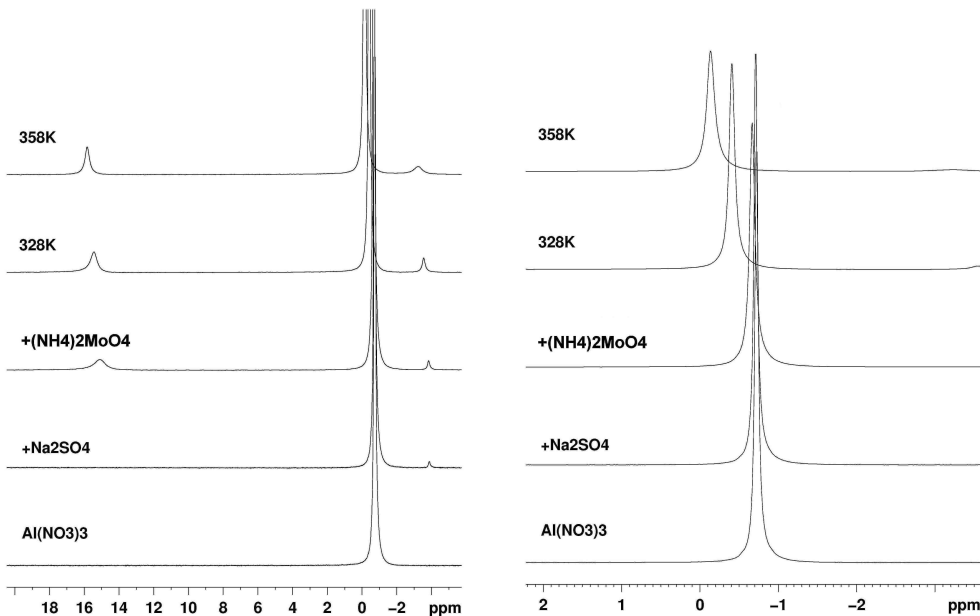


Fig. ESI 1: Left: Different ^{27}Al NMR spectra obtained after mixing stepwise aqueous solutions of $\text{Al}(\text{NO}_3)_3 \cdot 9\text{H}_2\text{O}$, $\text{Na}_2\text{SO}_4 \cdot 10\text{H}_2\text{O}$ and $(\text{NH}_4)_2\text{MoO}_4$ at room temperature and after heating (328, 358K) showing besides the signal of $[\text{Al}(\text{H}_2\text{O})_6]^{3+}$ those of **a** and **b** (see text above and original text). Right: Expansion of the area around 0 ppm demonstrates that the signal of $[\text{Al}(\text{H}_2\text{O})_6]^{3+}$ is shifted to *ca.* -0.2 ppm after heating. The other signal at -1 ppm (see Fig. 2 in the text) due to the presence of trapped $[\text{Al}(\text{H}_2\text{O})_6]^{3+}$ is of course missing.

2. Raman spectra and stability in solution

The bands of the two spectra of **1** and **2** (Fig. ESI 2 and 3) are due to vibrations of the molybdenum-oxide skeleton and are practically identical (apart from the expected facts that the lines in the solid state spectrum (Fig. ESI 3) are a little bit broader and the highest wavenumber band is only observed as a shoulder). The results show nicely that the same cluster skeleton is present in solutions and in crystals. (The shown spectra are only a few representatives among many others based on capsules with other ligands proving the same.) Referring to the aqueous solution of **1** it has been found that the spectrum does not change for a rather long time and this especially under exclusion of air. The intensities of the bands due to vibrations of the highly symmetrical spherical capsule skeleton are of course much higher than the intensities of the Raman bands of the other “parts”, like the ligands or $[\text{Al}(\text{H}_2\text{O})_6]^{3+}$; the latter are therefore not well observed under the present experimental conditions. Details will be published in due course.

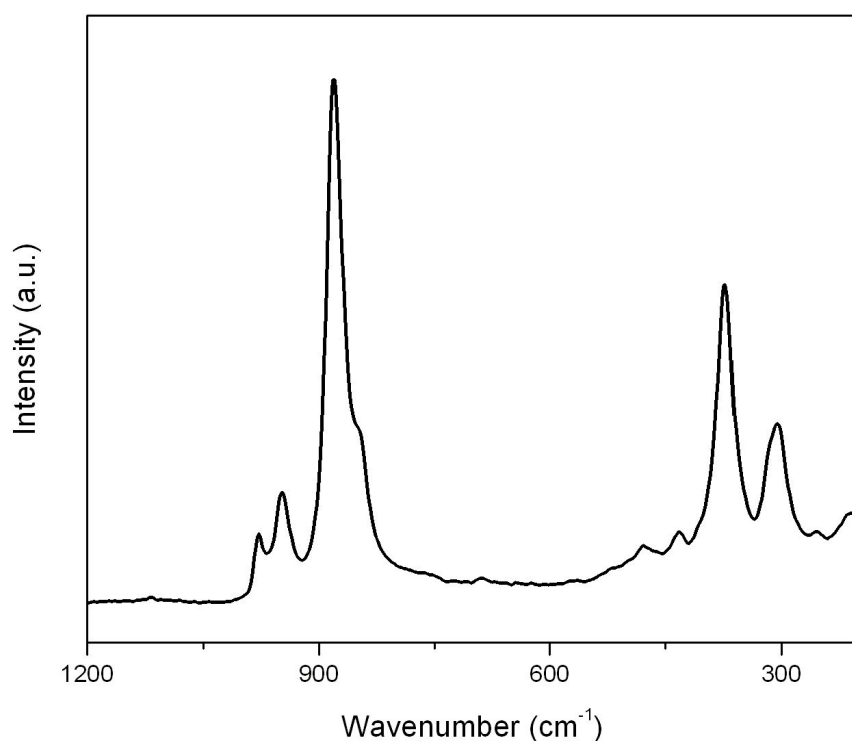


Fig. ESI 2: Raman spectrum of an aqueous solution of **1** ($\lambda_e = 1064 \text{ nm}$).

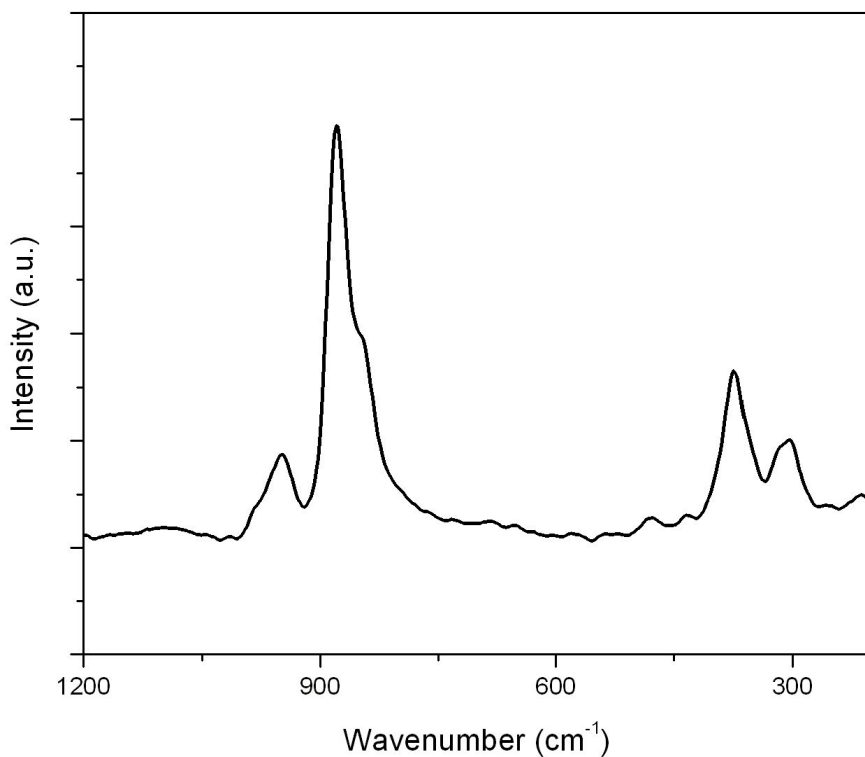


Fig. ESI 3: Solid-state Raman spectrum of **2** (KBr dilution; $\lambda_c = 1064$ nm).

We have the same situation for clusters where the sulphate ligands are replaced by others, e.g. by acetates, like for solutions of $(\text{NH}_4)_{42}[\text{Mo}^{\text{VI}}_{72}\text{Mo}^{\text{V}}_{60}\text{O}_{372}(\text{MeCO}_2)_{30}(\text{H}_2\text{O})_{72}] \cdot x\text{H}_2\text{O} \cdot y\text{MeCO}_2\text{NH}_4$ ($x \approx 300$, $y \approx 10$) **4** (see ref. 2a of the text). In this case the stability after a long exposure to air is even higher than in the sulphate case because of the smaller negative cluster charge. This has also been mentioned in the paper of S. Roy et al. (see footnote Δ), but in which the conditions for the deliberate oxidation of solutions of **4** were not mentioned (will be done shortly in an Addendum; private communication by W. Kegel).

3. Structures of water molecule assemblies encapsulated in the capsule cavities

The related structures depend on the type of pore closing (A. Müller, H. Bögge and E. Diemann, *Inorg. Chem. Comm.* 2003, **6**, 52; A. Müller, E. Krickemeyer, H. Bögge, M. Schmidtmann, S. Roy and A. Berkle, *Angew. Chem. Int. Ed.*, 2002, **41**, 3604; M. Henry, H. Bögge, E. Diemann and A. Müller, *J. Mol. Liq.*, 2005, **118**, 155), the type of coordinated ligands in the capsule as well as the presence/absence of integrated cations (see e.g. ref. 4 of the text). The special scenario of the encapsulation of a large $\{\text{H}_2\text{O}\}_{100}$ cluster filling the capsule cavity completely is of course only possible in absence of integrated cations. In the relevant compound case (space group $R\bar{3}m$) where the unit cell contains 12 formula units

(nine on 2/m sites, three on -3m sites) the structure of the water cluster is only nicely resolved on the lower symmetry site (see also J. Echeverría, D. Casanova, M. Llunell, P. Alemany, S. Alvarez, to be submitted to *Chem. Commun.*).

4. Acknowledgement

The authors gratefully acknowledge the financial support of the Deutsche Forschungsgemeinschaft (together with the U.S. National Science Foundation), the Fonds der Chemischen Industrie, the Volkswagenstiftung, the GIF and the European Union. A. Merca thanks the “Graduiertenkolleg Strukturbildungsprozesse”, Universität Bielefeld, for a fellowship.

Crystal data for 2: H₉₃₂ Al₁₉ Mo₁₃₂ N₁₅ O₉₂₈ S₃₀, $M = 30136.11 \text{ g mol}^{-1}$, space group C2/c, $a = 45.511(2)$, $b = 46.365(2)$, $c = 45.951(2) \text{ \AA}$, $\beta = 90.014(1)$, $V = 96961(8) \text{ \AA}^3$, $Z = 4$, $\rho = 2.064 \text{ g/cm}^3$, $\mu = 1.845 \text{ mm}^{-1}$, $F(000) = 58928$, crystal size = 0.3 x 0.25 x 0.2 mm³. A total of 290029 reflections ($1.54 < \Theta < 26.99^\circ$) were collected of which 105031 reflections were unique ($R(\text{int}) = 0.0466$). An empirical absorption correction using equivalent reflections was performed with the program SADABS 2.10. The structure was solved with the program SHELXS-97 and refined using SHELXL-97 to $R = 0.0633$ for 74506 reflections with $I > 2\sigma(I)$, $R = 0.1053$ for all reflections; max/min residual electron density 1.603 and -1.106 e Å⁻³. Crystals of 2 were removed from the mother liquor and immediately cooled to 188 (2) K on a Bruker AXS SMART diffractometer (three circle goniometer with 1K CCD detector, Mo-Kα radiation, graphite monochromator; hemisphere data collection in ω at 0.3° scan width in three runs with 606, 435 and 230 frames ($\Phi = 0, 88$ and 180°) at a detector distance of 5 cm). (SHELXS/L, SADABS from G.M. Sheldrick, University of Göttingen 1997/2003; structure graphics with DIAMOND 2.1 from K. Brandenburg, Crystal Impact GbR, Bonn, 2001.)